

## Effect of Thermal Treatment on the Heat of Vaporization of Bound Water by NMR and DSC Analysis

Yingjie Guo,<sup>a</sup> Minghui Zhang,<sup>b</sup> Yanjun Xie,<sup>a,\*</sup> Haiou Chen,<sup>a</sup> and Zefang Xiao<sup>a,\*</sup>

The vaporized heat of bound water in radiata pine wood sapwood, which was thermally treated at 200 °C, *via* N<sub>2</sub> protection for 24 h, were studied using low-field nuclear magnetic resonance (LFNMR) and differential scanning calorimetry (DSC) analysis. The bound water was divided into two states using LFNMR, which were absorbed water bonded with cell wall polymers and condensed bound water in the micro-pores of cell wall, respectively. The mass of the two states of bound water vaporized during DSC test was calculated based on the total mass of bound water vaporized and the moisture content of different water states in the water-saturated sapwood obtained, respectively. The reduction of moisture during DSC test was monitored synchronously using thermogravimetric analysis. The results showed thermal treatment decreased the spin-spin time ( $T_2$ ) of absorbed bound water and increased  $T_2$  of condensed bound water. The moisture content of the two states of bound water was reduced by thermal treatment. The vaporized heat of the bonded bound water was increased and that of the condensed bound water was reduced, which agreed with the change of  $T_2$  in the LFNMR experiment. The results suggest that bound water in the thermal treated wood is easier to vaporize when the relative humidity condition is more than 60%.

*Keywords:* Vaporized heat; Bound water; Thermal treatment; Radiata pine; Low field nuclear magnetic resonance; Differential scanning calorimetry; Thermogravimetric analysis

*Contact information:* a: Key Laboratory of Bio-Based Material Science and Technology (Ministry of Education), College of Material Science and Engineering, Northeast Forestry University, 26 Hexing Road, Harbin, 150040, People's Republic of China; b: Department of Material Science, Inner Mongolia Agricultural University, 306 Zhaowuda Road, Hohhot, 010018, People's Republic of China;

\* Corresponding author: xiaozefang@hotmail.com; yxie@nefu.edu.cn (Y. Xie).

### INTRODUCTION

Thermal treatment of wood is by far the most advanced commercial wood modification method. It induces chemical changes to the macromolecular constituents, resulting in a change in wood properties related to water, including the dimensional stability, mechanical properties, resistance to fungal decay and weathering, and coating of the wood. Bound water, existing in cell walls, has the greatest influence on the performance of wood (Hill 2006; Engelund *et al.* 2013; Čabalová *et al.* 2018; Dzurenda 2018). Thermal treatment changes the properties of bound water as well. Thermal treatment decreases the equilibrium moisture content (EMC) and the rate of moisture adsorption-desorption. It also reduces the effect of sorption hysteresis (Jalaludin *et al.* 2010a; Jalaludin *et al.* 2010b; Hill *et al.* 2012). The water states are influenced by thermal treatment as well, which can be detected by low field nuclear magnetic resonance (LFNMR) (Kekkonen *et al.* 2014).

The vaporized heat is a kind of bound water thermodynamics, which is related to

different stages of structural relaxation in wood during the desorption (Willems 2016). It can reflect the change of interaction energy between wood and water by thermal treatment. Although the change of vaporized heat of bound water due to modification methods was studied by theoretical calculation based on the sorption isotherms and Clausius-Clapeyron equation (Yasuda *et al.* 1995; Willems 2016), few studies have reported corresponding experimental findings.

The main objective of this study was to obtain the heat of vaporization bound water in thermally treated radiata pine (*Pinus radiata* D. Don) via differential scanning calorimetry (DSC) and thermogravimetric analysis (TG) instruments. The total heat of absorption was calculated based on heat flow measured by DSC and the mass of evaporated bound water was measured by TG. The LFNMR spin-spin time ( $T_2$ ) in water-saturated thermal-treated wood was recorded to provide the water state information which would be helpful to obtain the mass of bound water evaporated from DSC sample.

## EXPERIMENTAL

### Materials

#### *Thermal treated wood*

Radiata pine (*i.e.*, *Pinus radiata* D. Don) sapwood specimens was cut to 10 mm × 30 mm × 30 mm ( $L \times R \times L$ ) and thermally treated at a temperature of 200 °C under N<sub>2</sub> protection for 24 h. Nine replicates were required for both control and thermal-treatment group, respectively. The mass loss percent (MLP) of the samples was calculated using Eq. 1,

$$\text{MLP} = 100\% \times (m - m') / m \quad (1)$$

where  $m$  denotes the oven-dry mass of the sample before thermal-treated, and  $m'$  represents the oven-dry mass of the sample after thermal-treated.

#### *Nuclear magnetic resonance analysis*

Samples were cut into 9-mm-diameter cylinders (10 mm in length) and then were impregnated into distilled water using vacuum (0.01 MPa for 1 h) and pressure (0.6 MPa for 2 h). The water-saturated cylinders were placed into an NMR tube and analyzed at 40 °C using a time domain <sup>1</sup>H NMR (Bruker Minispec mq20, Berlin City, Germany), with a 0.7 Tesla permanent magnet (22.6 MHz proton resonance frequency). The  $T_2$  times were determined using the Carr-Purcell-Meiboom-Gill (CPMG) sequence with a pulse separation of  $\tau = 5$  ms, 5000 echoes, 16 scans, and a recycle delay of 2 s. The dead time was 4.8 μs. The Contin Laplacian transformation method was used to determine  $T_2$  distributions (Menon *et al.* 1987). The moisture content of various water states were calculated according the method reported by Telkki *et al.* (2013).

#### *Differential scanning calorimetry analysis*

After the LFNMR analysis, the control and thermal-treated cylinder samples were ground into 30-mesh particles, individually. Each type of particle sample was divided into three groups and the oven-dried mass was measured. After that, the samples were placed into three chambers with 40%, 60%, and 95% relative humidity (RH) at 30 °C. After 4 weeks, the equilibrium moisture content of each group was measured.

The heat of BW vaporization in each group was calculated using a DSC apparatus

(Q20, TA Instrument Company, New Castle, DE, USA) and a thermogravimetric analysis (TGA) instrument (Q50, TA Instrument Company, New Castle, DE, USA). Two sets of particle samples with equal masses ( $5 \pm 0.01$  mg) from the same group were placed in an unsealed DSC aluminum pan and a TGA sample plate. The DSC and TGA measurements began at the same time and shared the same heat-program, in which the temperature was raised at the rate of  $10 \text{ }^\circ\text{C min}^{-1}$  from  $25^\circ\text{C}$  to  $40 \text{ }^\circ\text{C}$ , and then maintained at  $40 \text{ }^\circ\text{C}$  for 30 min. And seven replicates were involved for both control and thermal-treatment.

#### *Heat of vaporization of bound water*

Both the heat flow and the change of mass were measured from 1.5 min. The method to calculate the vaporized heat of bound water is based on the assumption that BWI does not start to evaporate until all BWII has evaporated completely.

For each sample, the change of enthalpy was the sum of the heat absorbed by the sample plus the vaporized heat of the bound water absorbed with polymers of cell wall (BWI) and the heat of vaporization of the bound water condensed in micro-pores (BWII), as shown in Eq. 2,

$$\Delta H = Q_{\text{sample}} + Q_{\text{BWI}} + Q_{\text{BWII}} \quad (2)$$

where  $\Delta H$  represents the enthalpy change calculated by the heat flow curve;  $Q_{\text{sample}}$  represents the absorbed heat of the sample when the temperature increased from  $25$  to  $40 \text{ }^\circ\text{C}$ ; and  $Q_{\text{BWI}}$  and  $Q_{\text{BWII}}$  denote the absorbed heat of BWI and BWII evaporated from sample at  $40 \text{ }^\circ\text{C}$ , respectively. The  $Q_{\text{sample}}$ ,  $Q_{\text{BWI}}$ , and  $Q_{\text{BWII}}$  were calculated according to Eq. 3, 4, and 5, respectively,

$$Q_{\text{sample}} = C_{\text{wood}} \times m_1 \times (T_2 - T_1) \quad (3)$$

$$Q_{\text{BWI}} = H_{\text{V-BWI}} \times m_{\text{BWI}} \quad (4)$$

$$Q_{\text{BWII}} = H_{\text{V-BWII}} \times m_{\text{BWII}} \quad (5)$$

where  $C_{\text{wood}}$  represents the average specific heat capacity of wood ( $1.70 \text{ kJ}(\text{ kg}^\circ\text{C})^{-1}$ ) (Skaar 1988);  $m_1$  represents the mass measured by TG at 1.5 min;  $T_2$  is  $40 \text{ }^\circ\text{C}$ ;  $T_1$  is  $25 \text{ }^\circ\text{C}$ ;  $H_{\text{V-BWI}}$  is the vaporized heat per mass of BWI at  $40 \text{ }^\circ\text{C}$ ;  $m_{\text{BWI}}$  is the mass of BWI evaporated;  $H_{\text{V-BWII}}$  represents the vaporized heat per mass of BWII at  $40 \text{ }^\circ\text{C}$ ;  $m_{\text{BWII}}$  is the mass of BWII evaporated.

The initial moisture content of BWI ( $m'_{\text{BWI}}$ ) and BWII ( $m'_{\text{BWII}}$ ) in DSC sample at 1.5 min can be determined by the moisture content of the sample (MC) and the water-saturated moisture content of BWI ( $\text{MC}_{\text{NMR-BWI}}$ ) from LFNMR results. And both  $m_{\text{BWI}}$  and  $m_{\text{BWII}}$  can be determined.

If MC was less than or equal to  $\text{MC}_{\text{NMR-BWI}}$ ,  $m'_{\text{BWI}}$  was the MC and  $m'_{\text{BWII}}$  was zero. The  $H_{\text{V-BWI}}$  was calculated using Eq. 6

$$H_{\text{V-BWI}} = [\Delta H - Q_{\text{sample}}] / (m_1 - m_2) \quad (6)$$

where  $m_2$  denotes the final mass of the sample measured by TG; if MC was greater than  $\text{MC}_{\text{NMR-BWI}}$ ,  $m'_{\text{BWI}}$  was considered as  $\text{MC}_{\text{NMR-BWI}}$  and  $m'_{\text{BWII}}$  was the difference of MC minus  $\text{MC}_{\text{NMR-BWI}}$ .  $m'_{\text{BWII}}$  in DSC sample was calculated using Eq. 7

$$m'_{\text{BWII}} = m_0 \times (\text{MC} - \text{MC}_{\text{NMR-BWI}}) \quad (7)$$

where  $m_0$  is the dry mass of the DSC sample; if  $m'_{\text{BWII}}$  was greater than the mass of evaporated bound water, which indicated only BWII evaporated from the DSC sample, the  $H_{V\text{-BWII}}$  was calculated using Eq. 8

$$H_{V\text{-BWII}} = [\Delta H - Q_{\text{sample}}] / (m_1 - m_2) \quad (8)$$

If  $m'_{\text{BWII}}$  was less than the mass of vaporized bound water, both BWI and BWII were vaporized. It shows  $H_{V\text{-BWI}}$  and  $H_{V\text{-BWII}}$  was linearly expressed as Eq. 9:

$$0 = (m_1 - m_2 - m'_{\text{BWII}}) \times H_{V\text{-BWI}} + m'_{\text{BWII}} \times H_{V\text{-BWII}} - (\Delta H - Q_{\text{sample}}) \quad (9)$$

## RESULTS AND DISCUSSION

The radiata pine exhibited a mass loss of  $8.2 \pm 0.1\%$ , which is mainly attributed to the degradation of cell wall polymers (Hill 2006) at the heat treatment condition (Stamm 1956; Fung *et al.* 1974).

### Effect of Thermal Treatment on Water States

In the continuous  $T_2$  distributions of the control sample, there were four peaks (Fig. 1 control) suggesting four water states existed in the wood. The  $T_2$  value of peak 1 was  $1.3 \pm 0.2$  ms, which was similar to that of the previous studies and attributed to water bonded to hydroxyl groups of the polymers in the cell walls (BWI). The  $T_2$  value of peak 2 was  $4.9 \pm 0.7$  ms, which was attributed to the bound water condensed (BWII) in the micro-pores of cell wall.

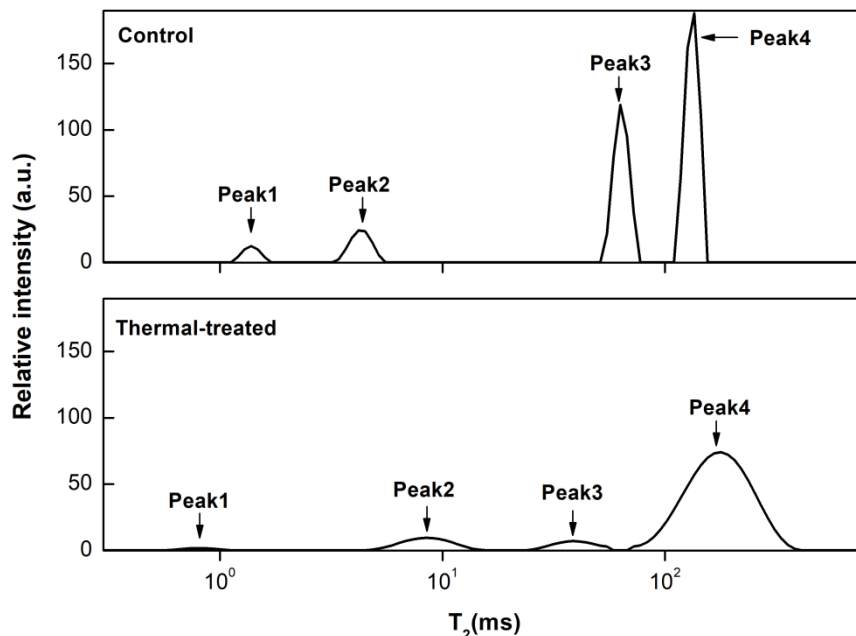


**Fig. 1.** The LFNMR  $T_2$  distributions for water states in the untreated control and thermal-treated wood

In some previous studies, the water state represented by the peak 2 was classified as free water in the volumes of smaller voids. However, those results are controversial because of the difficulty in separating the  $T_2$  of free water in the smaller voids from that

for bound water in the micropores of the cell walls. Peaks 3 and 4, in the range of 60 ms to 150 ms, were attributed to free water in the tracheid lumina of latewood and earlywood, respectively. (Thygesen and Elder 2008; Telkki *et al.* 2013; Fredriksson and Thygesen 2017; Gezici-Koç *et al.* 2017).

Compared with the control, the  $T_2$  distribution of the thermally treated sample also exhibited four peaks (Fig. 1). However, the values and the shapes of the relative peaks were clearly different from those of the control, which agreed with the results reported by Kekkonen *et al.* (2014). The shortened  $T_2$  for peak 1 ( $0.9 \pm 0.2$  ms) can be attributed to the reduction of hydrophilicity caused by the degradation of cell wall polymers (Hill 2006). The increased  $T_2$  of peak 2 ( $8.9 \pm 1.3$  ms) might be explained by the change of micro-pores' dimension caused by thermal-treatment. According to previous studies concerning the diameter of micro-pores in cell walls, it is mostly below 2.5 nm. In thermal treated wood, the range of micro-pore sizes is from 1.5 nm to 4.5 nm (Kekkonen *et al.* 2014). The shrinkage of the micro-pores (less than 2.5 nm) by thermal modification significantly hinders the access of water to the pores and the expanded micro-pores (more than 2.5 nm) are closer to the smaller voids of wood where free water exists. The change of  $T_2$  representing peak 3 and peak 4 reflected the change of the anatomical structure by thermal treatment (Fredriksson and Thygesen 2017)

### Effect of Thermal Treatment on Moisture Content of Water States

The MC for both kinds of BW was reduced by thermal treatment (Fig. 2). This was explained by a combination of the reduction of hydroxyl group and the change of micro-pore volumes. Because the sum of BWI and BWII can be considered as fiber saturated point (FSP), it can be concluded that thermal treatment reduced the wood FSP as well. These results agree with FSP reduction determined by several methods, including calculations with the Hailwood-Horrobin sorption model, interpreting moisture sorption isotherms of thermal-treated wood (RH 100%), and DSC investigations (Hill *et al.* 2012; Zelinka *et al.* 2012).

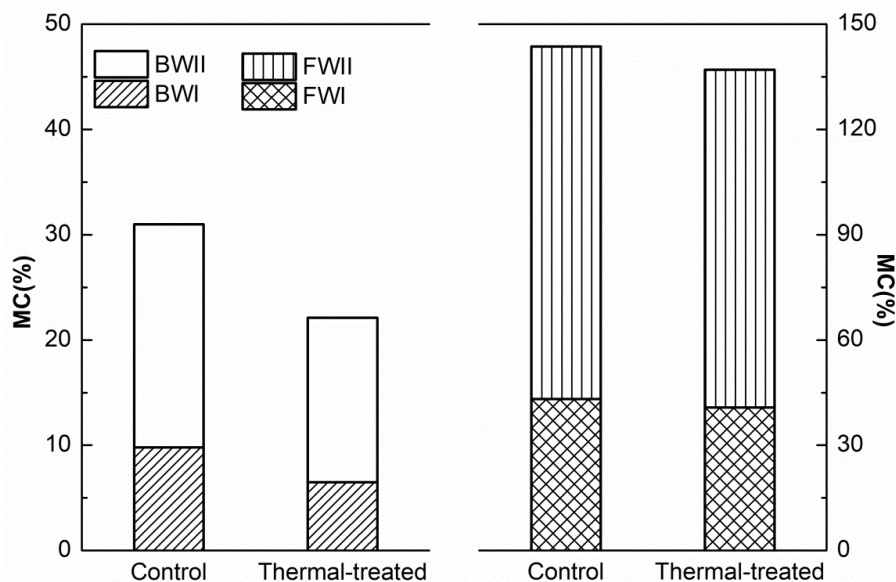


Fig. 2. The moisture content of different water states in saturated samples

The MC of free water represented by peaks 3 and 4 decreased in thermal group respectively, suggesting the reduction of free water in the wood anatomical structure by thermal treatment.

### Effect of Thermal Treatment on Heat Flow at 40 °C

For each group, the heat flow (HF) curves had a few features in common (Fig. 3). Each data curve was negative, which showed that the samples absorbed heat during bound water vaporization. The increase of the peaks with the growth of relative humidity suggested that the amount of BW evaporation affected the shape of the HF curve. Fluctuations were present in all the curves during the initial 0 to 1.5 min, with less amplitude for increasing MC's. This could be due to the effects of moisture on the heat transformation in wood. (Skaar 1988).

For both untreated and thermal-treated samples (Fig. 3a), the amplitude of HF increased with the growth of RH, which could be attributed to the rise of moisture content in wood. However, the amplitude of HF increased less in thermal-treated group, suggesting the less increased moisture content by thermal treatment. This change of moisture content led to the decreased amplitude in thermal group when both groups were under the same relative humidity conditions.

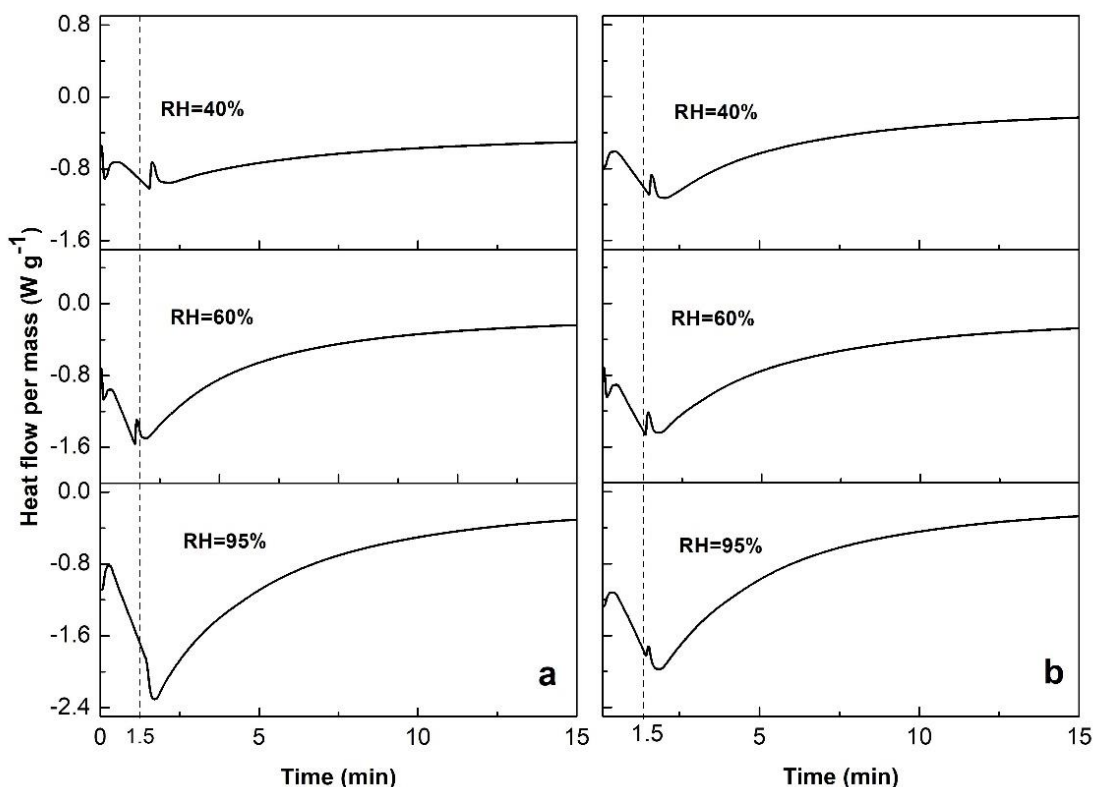


Fig. 3. Heat flow per unit mass at 40 °C for the untreated control (a) and thermal-treated wood (b)

### Effect of Thermal Treatment on the Heat of Vaporization of Bound Water at 40 °C

For both the control and the thermal-treated groups, the vaporization heat of BWI in the cell walls was able to be calculated when conditioned at 40% and 60% RH (Table 1). When the RH was increased to 95%, the moisture content of both groups after DSC measurement was still higher than the maximum BWI (obtained by NMR), resulting in

the impossibility of calculation of the vaporized heat of BWI. Conditioned under 60 and 95% RH, the heat of vaporization of BWII was lower than that of BWI, suggesting the weaker interaction of BWII with the cell walls. Besides, the increased RH did not influence the vaporization heat of both BWI and BWII, which agreed with the results of the comparable thermodynamics of bound water calculated based on sorption isotherms and the Clausius-Clapeyron equation (Skaar 1988; Willems 2014).

The vaporized heat of BWI in the thermal-treated sample was slightly higher than that in the untreated wood; and the heat of vaporization of BWII was less than that in the control, which agreed with the results for  $T_2$  in the LFNMR experiment. The higher vaporized heat of BWII indicated that less heat was needed for BWII to reach equilibrium during the desorption process. This can be explained by the change of micro-pore dimensions. When the bound water evaporates from the cell walls, it might require less energy to escape from the expended micro-pores by thermal treatment. This result indicates that moisture in the thermal treated wood is easier to desorb when the relative humidity condition is more than 60%.

**Table 1.** Bound Water Moisture Content ( $MC_{\text{bound}}$ ) after Conditioning under Various RH, the Vaporized Moisture Content after DSC Test ( $MC_{\text{vaporized}}$ ), Moisture Content of Adsorbed Water in Cell Wall at Fiber Saturation Point Measured Using LFNMR ( $MC_{\text{NMR-BWI}}$ ), Vaporization Heat of Adsorbed Water ( $H_{V\text{-BWI}}$  Calculated by Eq. 6) and Vaporization Heat of Water Condensed in Micropores ( $H_{V\text{-BWII}}$  Calculated by Eq. 8) in the Control and Thermal-treat Groups

	Mass Loss (%)	RH (%)	$MC_{\text{bound}}$ (%)	$MC_{\text{vaporized}}$ (%)	$MC_{\text{NMR-BWI}}$ (%)	$H_{V\text{-BWI}}$ ( $\text{kJ kg}^{-1}$ )	$H_{V\text{-BWII}}$ ( $\text{kJ kg}^{-1}$ )
Control	0	40	$6.4 \pm 0.2$	$2.1 \pm 0.1$	$9.8 \pm 0.2$	$47.4 \pm 3.3$	—
		60	$10.9 \pm 1.1$	$5.1 \pm 0.1$		$47.4 \pm 3.3$	$39.9 \pm 3.4$
		95	$19.8 \pm 0.8$	$9.9 \pm 0.2$		—	$40.3 \pm 1.5$
Thermal	$8.2 \pm 0.1$	40	$5.4 \pm 0.6$	$1.8 \pm 0.3$	$5.7 \pm 0.8$	$48.8 \pm 1.3$	—
		60	$8.5 \pm 0.7$	$2.7 \pm 0.2$		$48.8 \pm 1.3$	$34.9 \pm 2.4$
		95	$15.4 \pm 1.1$	$5.4 \pm 1.1$		—	$35.0 \pm 1.4$

## CONCLUSIONS

1. The heat of vaporization of the absorbed bound water is higher than that of the condensed bound water, suggesting the easier evaporation of condensed bound water during the desorption process.
2. Thermal treatment slightly increased the heat of vaporization of absorbed bound water, which could be credited to degradation of chemical components in cell walls. The reduction of vaporization heat of condensed bound water could be due to the change of micropore sizes, which was also caused by the aforementioned degradation.
3. The heat of vaporization of the two states of bound water was irrelevant to the

increased relative humidity. However, it may be related to the degree of the degradation by thermal treatment.

## ACKNOWLEDGMENTS

The authors are grateful for the support from the National Natural Science Foundations of China (31500469 & 31470585).

## REFERENCES CITED

- Čabalová, I., Kačík, F., Lagana, R., Výbohová, E., Bubeníková, T., Čaňová, I., and Ďurkovič, J. (2018). "Effect of thermal treatment on the chemical, physical, and mechanical properties of pedunculate oak (*Quercus robur* L.) wood," *BioResources* 13(1), 157-170. DOI: 10.15376/biores.13.1.157-170
- Dzurenda, L. (2018). "The shades of color of *Quercus robur* L. wood obtained through the processes of thermal treatment with saturated water vapor," *BioResources* 13(1), 1525-1533. DOI: 10.15376/biores.13.1.1525-1533
- Engelund, E. T., Thygesen, L. G., Svensson, S., and Hill, C. A. S. (2013). "A critical discussion of the physics of wood-water interactions," *Wood Science and Technology* 47(1), 141-161. DOI: 10.1007/s00226-012-0514-7
- Fredriksson, M., and Thygesen, L. G. (2017). "The states of water in Norway spruce (*Picea abies* (L.) Karst.) studied by low-field nuclear magnetic resonance (LFNMR) relaxometry: Assignment of free-water populations based on quantitative wood anatomy," *Holzforschung* 71(1), 77-90. DOI: 10.1515/hf-2016-0044
- Fung, D. P. C., Stevenson, J. A., and Shields, J. K. (1974). "The effect of heat and  $\text{NH}_4\text{H}_2\text{PO}_4$  on the dimensional and anatomical properties of Douglas fir," *Wood Science* 7(1), 13-20.
- Gezici-Koç, Ö., Erich, S. J. F., Huinink, H. P., Ven, L. G. J. V., and Adan, O. C. G. (2017). "Bound and free water distribution in wood during water uptake and drying as measured by  $^1\text{D}$  magnetic resonance imaging," *Cellulose* 24(2), 535-553. DOI: 10.1007/s10570-016-1173-x
- Hill, C. A. S. (2006). "Thermal modification of wood," in: *Wood Modification: Chemical, Thermal and Other Processes*, C. V. Stevens (ed.), John Wiley & Sons Ltd., West Sussex, England, pp. 99-127.
- Hill, C. A. S., Ramsay, J., Keating, B., Laine, K., Rautkari, L., Hughes, M., and Constant, B. (2012). "The water vapour sorption properties thermally modified and densified wood," *Journal of Materials Science* 47(7), 3191-3197. DOI: 10.1007/s10853-011-6154-8
- Jalaludin, Z., Hill, C. A. S., Samsi, H. W., Husain, H., and Xie, Y. (2010a). "Analysis of water vapour sorption of oleo-thermal modified wood of *Acacia mangium* and *Endospermum malaccense* by a parallel exponential kinetics model and according to the Hailwood-Horrobin model," *Holzforschung* 64(6), 763-770. DOI: 10.1515/HF.2010.100
- Jalaludin, Z., Hill, C. A. S., Samsi, H. W., Husain, H., Xie, Y., Awang, K., and Curling, S. F. (2010b). "Analysis of the water vapour sorption isotherms of thermally modified *Acacia* and sesendok," *Wood Material Science and Engineering* 5(3), 194-203. DOI:



10.1080/17480272.2010.503940

- Kekkonen, P. M., Ylisassi, A., and Telkki, V.-V. (2014). "Absorption of water in thermally modified pine wood as studied by nuclear magnetic resonance," *The Journal of Physical Chemical C* 118(4), 2146-2153. DOI: 10.1021/jp411199r
- Menon, R. S., Mackay, A. L., Hailey, J. R. T., Bloom, M., Burgess, A. E., and Swanson, J. S. (1987). "An NMR determination of the physiological water distribution in wood during drying," *Journal of Applied Polymer Science* 33(4), 1141-1155. DOI: 10.1002/app.1987.070330408
- Skaar, C. (1988). "Moisture sorption thermodynamics," in: *Wood and Water Relations*, Springer-Verlag, Heidelberg, Berlin, pp. 46-85.
- Stamm, A. J. (1956). "Thermal degradation of wood and cellulose," *Industrial and Engineering Chemistry* 48(3), 413-417. DOI: 10.1021/ie51398a022
- Telkki, V.-V., Yliniemi, M., and Jokisaari, J. (2013). "Moisture in softwoods: Fiber saturation point, hydroxyl site content, and the amount of micropores as determined from NMR relaxation time distributions," *Holzforschung* 67(3), 291-300. DOI: 10.1515/hf-2012-0057
- Thygesen, L. G., and Elder, T. (2008). "Moisture in untreated, acetylated, and furfurylated Norway spruce studied during drying using time domain NMR," *Wood and Fiber Science* 40(3), 309-320.
- Willems, W. (2014). "Hydrostatic pressure and temperature dependence of wood moisture sorption isotherms," *Wood Sci Technol* 48, 483-498. DOI 10.1007/s00226-014-0616-5
- Willems, W. (2016). "Equilibrium thermodynamics of wood moisture revisited: presentation of a simplified theory," *Holzforschung* 70(10), 963-970. DOI: 10.1515/hf-2015-0251
- Yasuda, R., Minato, K., and Norimoto, M. (1995). "Moisture adsorption thermodynamics of chemically modified wood," *Holzforschung* 49(6), 548-554. DOI: 10.1515/hfsg.1995.49.6.548
- Zelinka, S. L., Lambrecht, M. J., Glass, S. V., Wiedenhoeft, A. C., and Yelle, D. J. (2012). "Examination of water phase transitions in loblolly pine and cell wall components by differential scanning calorimetry," *Thermochimica Acta* 533, 39-45. DOI: 10.1016/j.tca.2012.01.015

Article submitted: January 16, 2018; Peer review completed: March 25, 2018; Revised version received and accepted: May 21, 2018; Published: June 4, 2018.  
DOI: 10.15376/biores.13.3.5534-5542